Halme, Janne; Mäkinen, Pyry

# Theoretical efficiency limits of ideal coloured opaque photovoltaics

*Published in:*
Energy and Environmental Science

*DOI:*
10.1039/c8ee03161d

Published: 01/04/2019

*Document Version*
Peer-reviewed accepted author manuscript, also known as Final accepted manuscript or Post-print

*Please cite the original version:*
Halme, J., & Mäkinen, P. (2019). Theoretical efficiency limits of ideal coloured opaque photovoltaics. *Energy and Environmental Science*, *12*(4), 1274-1285. https://doi.org/10.1039/c8ee03161d

# Theoretical efficiency limits of ideal coloured opaque photovoltaics

Janne Halme*[1] and Pyry Mäkinen[1]

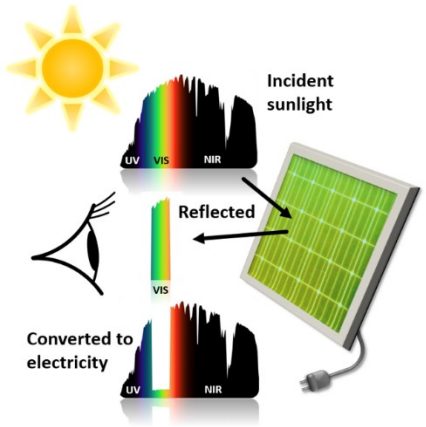


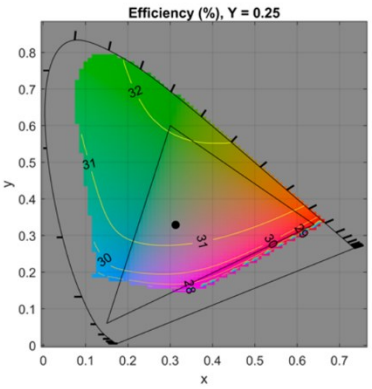


Theoretical analysis connecting photovoltaics and colorimetry reveals the ultimate efficiency limits of colorful single-band-gap solar cells and modules.


## Abstract

Colour can improve the visual aesthetics of solar cells for building and product integration but constitutes an optical loss from the perspective of photovoltaic energy conversion. To quantify this compromise, we report the theoretical efficiency limits of ideal coloured opaque single-band-gap solar cells. The colours were optimized by allowing the solar cells to reflect light within two distinct wavelength bands in the visible region. Colour chromaticity and brightness were controlled by modifying the position and width of the reflection bands, while optimising the band-gap energy for each colour. We found that almost the entire sRGB colour space has an efficiency limit greater than 29 %, when relative luminosity is less than 0.25. This corresponds to a relative performance loss of less than 14% compared to an ideal black solar cell. Yellow-green is the most efficient photovoltaic colour, whereas highly saturated blue, red and purple colours produce the lowest efficiencies, when compared at equal brightness. The colour-dependence is explained by the photopic sensitivity of the human eye, which peaks at yellow-green wavelengths and tails towards the blue and red ends of the visible spectrum. For most colours, except the darkest ones, the optimal band-gap energy for a theoretically ideal solar cell is between 1.115 eV and 1.135 eV, matching the value for crystalline silicon. The results clarify the link between the solar cell colour and efficiency and establish a reference point and guidelines for optimizing coloured photovoltaics.


## Broader context

At present, about 40% of the energy demand worldwide is consumed in buildings. Enhancing their energy efficiency is therefore important for mitigating climate change. Building-integrated photovoltaic energy systems could theoretically provide electricity to buildings at low cost, because the integrated solar modules can double as construction materials like façade claddings and roof tiles, potentially lowering overall construction costs. This is particularly important for increasing solar energy utilization in densely built areas where traditional ground-mounted photovoltaic installations cannot be easily used. Integration of photovoltaic elements on the building skin nevertheless requires that their visual appearance, like surface texture and colour, is compatible with the other building materials. Both industry and academia are therefore developing coloured solar modules for solar architecture. Because the colour of the solar cell is produced by reflection of visible light from its surface, it decreases the energy conversion efficiency of the cell compared to a black cell that would absorb and convert this light to electricity. Here, we determined the maximum efficiency that a coloured solar cell can theoretically have, when the colour is formed in an energetically optimal way. Linking photovoltaics to colorimetry, the results provide a theoretical reference point for optimizing coloured photovoltaics.

[1] Department of Applied Physics, Aalto University School of Science, P.O. Box 15100, 00076 Aalto, Finland. E-mail: janne.halme@aalto.fi. Electronic Supplementary Information is available.

# Introduction

Photovoltaic modules are normally used in ground-mounted solar power plants or roof-top photovoltaic (PV) installations with the aim of producing solar electricity at the lowest possible cost. However, there is increasing interest in the visual aesthetics of the solar modules for particular PV applications. For example, in building-integrated photovoltaics (BIPV), façade installation offers a large additional surface area for solar electricity generation, but requires solar modules whose colour, texture or transparency meet architectural requirements.[1–3] Aesthetically designed solar cells are also needed for product-integrated photovoltaics (PIPV), where solar cells can provide low-power electronics with energy-autonomous operation or extended battery life, but must at the same time match the overall visual design of the product.[4,5]

The colour of solar cells can originate from the solar cell absorber materials themselves, or from additional optical materials and coatings applied to them. For example, organic[6], dye-sensitized[7–9] and perovskite[10,11] solar cells offer various colour options due to the wavelength-dependent visible light absorption characteristics of their active materials, whereas inherently black crystalline silicon[12–14], CIGS[15] and CdTe[16] solar cells can be rendered colourful by depositing additional coloured materials or photonic structures on them. Although the majority of the scientific literature on coloured photovoltaics has focused on semi-transparent solar cells[17,18], the combination of transparency and colour is rare in conventional architecture, which suggests that aesthetic building integration mainly calls for coloured opaque (walls and roofs) or achromatic transparent[19,20] (windows, skylights and glass facades) PV modules. Our focus in this paper is therefore on opaque coloured solar cells.

Opaque solar cells can be coloured, for example, with modified antireflective coatings[12–14], distributed Bragg reflectors[15,21], resonant dielectric nanoscatterers[22], plasmonic particles[23] and structures[24], or luminescent materials[16] that reflect or emit coloured light. Moreover, the visual appearance of conventional opaque solar modules can be modified with coloured optical coatings or materials applied on their front glass[21,25,26] or encapsulation polymer layer[16]. This hides the underlying solar cells visually while producing the desired coloured appearance that can be uniform, patterned, textured, or even consist of colour-printed graphics, to mimic conventional building materials[27–30] or to create photovoltaic visual art and design[31,32].

Because the colour of a solar cell is produced by visible light that is either reflected from or transmitted through the cell, it constitutes an optical loss from the perspective of photovoltaic solar energy conversion. To find the best compromise between efficiency and aesthetics, the required colour hue and brightness must be formed in a way that minimizes unnecessary optical losses while maximizing photovoltaic efficiency. Although this general principle is qualitatively well understood, and has motivated the above-mentioned experimental investigations, there have been few theoretical studies on the influence of colour on photovoltaic efficiency. Moreover, the previous studies have been limited to one photovoltaic technology and assumed non-ideal solar cell models with at least some unoptimized experimental parameters values. Forberich et al. studied the interplay of colour and efficiency in semi-transparent organic solar cells that were subject to practical performance limitations specific to organic photovoltaic materials.[33] Peharz and Ulm calculated the influence of colours on the performance of crystalline silicon solar cells, by simulating their current-voltage curve with a two-diode model based on experimentally determined dark saturation current densities.[34] These studies leave open the fundamental question: what is the ultimate theoretical efficiency limit of a solar cell that has certain colour?

Here, we answer this question by calculating the theoretical efficiency limits of coloured photovoltaics, by considering an ideal single-band-gap solar cell and energy-wise optimal colours, without making any PV-technology-specific empirical assumptions. Moreover, to arrive at fundamental efficiency limits, we specifically neglect all other (parasitic) optical losses than those required to form the solar cell colour in an energetically optimal way. In an earlier study, Lunt determined the corresponding efficiency limits for visibly

transparent achromatic solar cells, showing that the limit for a visibly fully transparent single-band-gap solar cell is 20.6 %, which is ca 2/3 of the 33.1 % theoretical limit for corresponding opaque black solar cells.[35] Here, we extend this theoretical analysis to coloured solar cells, and show that almost the entire sRGB colour space has a single-bandgap efficiency limit of over 29%, which corresponds to a relative performance loss of below 14% compared to an ideal black solar cell. The results quantify the fundamental interdependence between colour and efficiency in solar cells, reveal yellow-green as the most efficient solar cell colour, and provide the understanding necessary to instruct performance optimization of coloured photovoltaics.

The results are valid as theoretical limits for all types of single-junction solar cells that are based on a single absorber material characterized by a single band gap energy, such as crystalline silicon solar cells, organic solar cells, dye-sensitized solar cells and organometal halide perovskite solar cells. Althought calculated for opaque solar cells, the theoretical efficiencies serve also as upper limits for semi-transparent coloured cells.

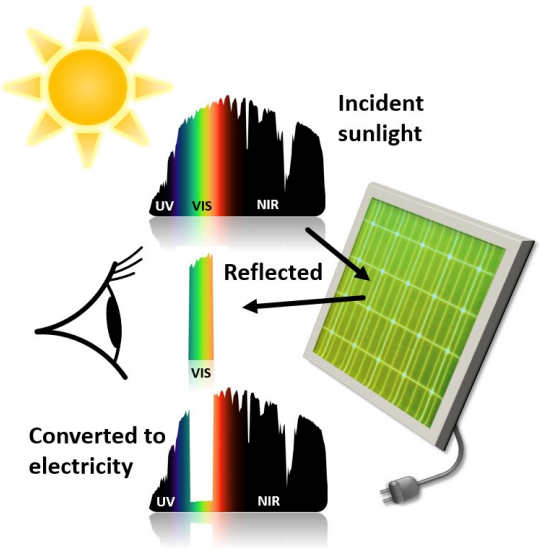


Fig. 1. An ideal coloured opaque solar cell reflects some fraction of the visible (VIS) sunlight while absorbing and converting to electricity the ultraviolet (UV) and near-infrared (NIR) parts of the solar spectrum.

# Theory

## Calculation of the theoretical efficiency limit

The theoretical efficiency limits are calculated according to the detailed balance limit originally presented by Shockley and Queisser[36] and recently updated to the standard test conditions by Rühle[37]. According to the model, the current-voltage (JV) curve of the solar cell is given by

$$J(V) = J_{ph} - J_{rec}(V) \quad (1)$$

where $J_{ph}$ is the photocurrent density and $J_{rec}$ is the recombination current density. In this case, the photocurrent density equals the short-circuit current density $J_{sc}$, because additional loss factors such as series resistance are omitted and charge carrier diffusion lengths are assumed infinite. $J_{ph}$ is calculated as

$$J_{ph} = q\int_{E_g}^{\infty} EQE(E)S(E)dE = q\int_{0}^{\lambda_g} EQE(\lambda)S(\lambda)d\lambda \quad (2)$$

where $S$ is the photon flux per unit area incident on the solar cell, in this case the AM1.5G standard solar spectrum normalized to 1000 W/m$^2$ total irradiance, $EQE$ is the external quantum efficiency of the cell, $\lambda_g$ is the light wavelength at the absorption edge corresponding to the band-gap energy $E_g$ ($\lambda_g = hc/E_g$) and $q$ is

the elementary charge. It is assumed that the solar cell is planar, and the photon flux is incident on it in the direction of its surface normal.

The external quantum efficiency (*EQE*) of any coloured opaque solar cell can be written in a general case as

$$EQE(\lambda) = \begin{cases} [1 - R(\lambda) - A_{loss}(\lambda)]IQE(\lambda) & , 0 < \lambda \leq \lambda_g \\ 0 & , \lambda > \lambda_g \end{cases} \quad (3)$$

where $R(\lambda)$ is the total hemispherical spectral reflectance of the solar cell, hereafter called 'reflectance', $A_{loss}(\lambda)$ is the parasitic absorption loss in the solar cell, and $IQE(\lambda)$ is the internal quantum efficiency of the cell. Nevertheless, an *ideal coloured opaque solar cell* has no parasitic absorption losses, and its *IQE* = 1 for all wavelengths below $\lambda_g$, omitting the possibility for multiple carrier generation.[38] When other complex mechanisms like up-conversion[39], down-conversion[40] and intermediate band effects[41] are also omitted, the *EQE* of an ideal coloured opaque solar cell is defined solely by its optical reflectance:

$$EQE(\lambda) = \begin{cases} 1 - R(\lambda) & , 0 < \lambda \leq \lambda_g \\ 0 & , \lambda > \lambda_g \end{cases} \quad \text{(for ideal coloured opaque solar cell)} \quad (4)$$

This ideal condition can be approached in practice for example with highly efficient black solar cells equipped with an optical coating or cover that exhibits wavelength-selective visible reflection but does not itself absorb any photons above the band-gap energy of the underlying solar cell. The same ideal condition is nevertheless valid as a theoretical limit for all kinds of solar cells, regardless of the way how their colour is produced.

The recombination current density can be approximated with the diode equation[42,43]

$$J_{rec}(V) = J_{rec0}\left(e^{\frac{qV}{kT}} - 1\right) \quad (5)$$

where the $J_{rec0}$ is the recombination current density without bias ($V$ = 0) when the cell is in the dark in thermal equilibrium with its surroundings at temperature $T$ = 298.15 K (25 °C), and $k$ is the Boltzmann's constant. At the SQ limit, the only recombination mechanism is radiative recombination.[36] According to the detailed balance, the radiative recombination rate equals the rate of absorption and carrier generation at each photon energy $E$, and can therefore be calculated using the black body radiation spectrum at temperature $T$, when the absorptance $A(E)$ of the solar cell is known. The recombination current density at equilibrium in the dark is therefore

$$J_{rec0} = rqp_{rad0} \quad (6)$$

where $p_{rad0}$ is the rate of photon emission to the surroundings per unit area, given by[42]

$$p_{rad0} = \frac{2\pi}{h^3c^2}\int_0^\infty A(E)E^2e^{-\frac{E}{kT}}dE = \frac{2\pi}{h^3c^2}\int_{E_g}^\infty [1 - R(E)]E^2e^{-\frac{E}{kT}}dE \quad (7)$$

where $c$ is the speed of light in vacuum. Note that $A(E) = EQE(E) = 1 - R(E)$ was introduced in equation (7), because at the theoretical limit all the photons that are absorbed are converted to photocurrent in the cell, whereas all the photons that are not absorbed are reflected from the cell.

The factor $r$ is used in equation (6) to normalize the thermal emission and absorption rate to the area exposed to sunlight. If the solar cell is equipped with a perfect back-reflector, $r$ = 1 because only the front of the solar cell emits and absorbs thermal radiation at temperature $T$, i.e. the area is the same as that used for absorbing sunlight. Without a back-reflector, $r$ = 2 because the back of the cell is also available for emission and absorption of thermal radiation. A perfect back-reflector thus increases the theoretical efficiency by halving the probability for radiative recombination events in the cell. Because in this work we consider only coloured

opaque solar cells, we use $r$ = 1. Nevertheless, for the above-mentioned reason, the results also represent the upper limits for coloured semi-transparent solar cells of corresponding transmitted light color and brightness.

The efficiency of the solar cell was obtained by finding the voltage that maximizes the output power density of the cell $[J(V)V]_{max}$ at the given incident total solar irradiance of $P_{in}$ = 1000 W/m$^2$

$$\eta = [J(V)V]_{max}/P_{in} \tag{8}$$

The fill factor of the solar cell JV-curve is

$$FF = J_{mpp}V_{mpp}/J_{SC}V_{OC} \tag{9}$$

where $J_{SC}$ and $V_{OC}$ are the short-circuit current density and open circuit voltage, and $J_{mpp}$ and $V_{mpp}$ their values at the maximum power point (MPP).

It can be seen from the above equations that the colour of the solar cell, i.e. its spectral reflectance, affects both the photocurrent density $J_{ph}$ (equations 2 and 4) and the recombination current density $J_{rec0}$ (equations 5 – 7) roughly proportionally. However, the effect through $J_{ph}$ has more influence on cell efficiency, because $J_{ph}$ affects $J_{sc}$ linearly, whereas $J_{rec0}$ affects $V_{OC}$ logarithmically. For example, increasing reflectance from 0 % to 50 % throughout the absorbed UV-VIS-NIR wavelength region would halve $J_{ph}$ and thereby efficiency, whereas a concomitant 50 % drop in $J_{rec0}$ would only increase efficiency by 2 % in relative terms. In our case, the effect through $J_{rec0}$ is even smaller, because we change reflectance only in the visible region where the thermal emission from the cell is much weaker than in the NIR region, as determined by the black body radiation spectrum at $T$ = 298.15 K. The effect of colour on solar cell efficiency can therefore be safely discussed in terms of photocurrent generation only.

## Colour model

Human colour perception is represented quantitatively by the CIE 1931 XYZ standard that describes colours with $X$-, $Y$- and $Z$-coordinates, also known as XYZ tri-stimulus values[44,45]

$$X = \frac{\int_{360\ \mathrm{nm}}^{830\ \mathrm{nm}} R(\lambda)P(\lambda)\bar{x}(\lambda)d\lambda}{\int_{360\ \mathrm{nm}}^{830\ \mathrm{nm}} P(\lambda)\bar{y}(\lambda)d\lambda} \tag{10}$$

$$Y = \frac{\int_{360\ \mathrm{nm}}^{830\ \mathrm{nm}} R(\lambda)P(\lambda)\bar{y}(\lambda)d\lambda}{\int_{360\ \mathrm{nm}}^{830\ \mathrm{nm}} P(\lambda)\bar{y}(\lambda)d\lambda} \tag{11}$$

$$Z = \frac{\int_{360\ \mathrm{nm}}^{830\ \mathrm{nm}} R(\lambda)P(\lambda)\bar{z}(\lambda)d\lambda}{\int_{360\ \mathrm{nm}}^{830\ \mathrm{nm}} P(\lambda)\bar{y}(\lambda)d\lambda} \tag{12}$$

where $\bar{x}$, $\bar{y}$ and $\bar{z}$ are the colour-matching functions of the CIE standard observer[46], $P(\lambda)$ is AM1.5G 1000 W/m$^2$ spectral solar irradiance ($P(\lambda) = S(\lambda)hc/\lambda$) and $R(\lambda)$ is the spectral reflectance of the solar cell (Fig. 2a). The $\bar{x}$, $\bar{y}$ and $\bar{z}$ functions represent roughly the red, green and blue colour sensation, respectively.[45] In equations 10 – 12, the XYZ-coordinates are normalized with the maximum $Y$ coordinate value. The normalized $Y$ takes values between 0 and 1, where $Y$ = 0 corresponds to a perfectly black solar cell and $Y$ = 1 to a perfectly white solar cell, black meaning complete absorption and white complete reflection of the visible light from 360 nm to 830 nm, respectively. The normalized $Y$ coordinate is called *relative luminosity*. The relative luminosity is also known as *average visible reflectance* (AVR) and is a property equivalent to *average visible transmittance* (AVT) used in the context of semi-transparent solar cells.

The colours were transformed into the CIE xyY colour space by calculating their $x$ and $y$ chromaticity coordinates as

$$x = \frac{X}{X+Y+Z} \quad (13)$$

$$y = \frac{Y}{X+Y+Z} \quad (14)$$

This facilitated comparison of the efficiency limits of different colours at equal relative luminosity (*Y*-value) in the CIE 1931 chromaticity diagram. For presentation in figures, the XYZ-coordinates were further transformed into the sRGB colour space using CIE D65 spectrum as the standard white, which corresponds roughly to the solar illumination in Western and Northern Europe at noon. The RGB-coordinates were normalized with the D65 spectrum so that their maximum value ([R,B,G] = [1,1,1]) corresponds to the XYZ-coordinates of the D65 illuminant ([X,Y,Z] = [0.95047, 1, 1.08883]).

## Optimal colour formation principle

The efficiency of an ideal coloured solar cell is maximal when the colour is produced by reflecting as few photons as possible that could be otherwise be converted into electricity in the cell. In practice, the optimal way to reach this condition depends on the spectral features of the incident light, the reflectance and parasitic absorptance by the solar cell, the internal quantum efficiency of the solar cell, and on human colour perception. However, when it comes to the theoretical efficiency limits of an ideal coloured opaque solar cell, characterized by $A_{loss}(\lambda) = 0$ and $IQE(\lambda) = 1$, the solar cell reflectance and the incident light spectrum have no effect on colour optimization because they affect both photocurrent generation (equations 2 and 4) and the colour coordinates (equations 10 – 12) proportionally. This leaves human colour perception as the only decisive factor and leads to an optimal colour formation principle that described in detail in Electronic Supplementary Information.

At the theoretical efficiency limit, the principle for optimal colour formation is to reflect primarily wavelengths near the peaks of the colour-matching functions (Fig. 2a), or more precisely, near the peaks of the wavelength-normalized colour-matching functions, $\bar{x}/\lambda$, $\bar{y}/\lambda$ and $\bar{z}/\lambda$ . In this way, a minimal number of incident photons are wasted, in photovoltaic terms, for generating colour instead of photocurrent. This principle is justified in detail in the Electronic Supplementary Information.

Following the principle, the colours were formed optimally by allowing the solar cell to reflect two narrow wavelength bands, corresponding to two rectangular dips in the *EQE* spectrum (Fig. 2a).[47] The bands are characterized by their lower and higher cut-off limits, $\lambda_{low}$ and $\lambda_{high}$, and $EQE = 0$ and $R = 1$ between them ($EQE = 1 - R$). Outside the bands, all photons are absorbed, i.e. $EQE = 1$ and $R = 0$, except that *EQE* is zero for all photon energies below the band-gap energy $E_g$ ($\lambda > \lambda_g$). The resulting colours were identified by calculating their XYZ coordinates with equations 10 – 12.

Note that 100 % reflectance within the bands allows them to be as narrow as possible, which maximizes the utilization of the most optimal band position, leading to energy-wise optimal colour formation and maximal cell efficiency. This principle is consistent with the seminal works of Schrödinger and MacAdam who studied the maximal luminous efficiency of coloured materials.[48,49] We note here that in their colour optimization algorithm, Peharz and Ulm had allowed less than 100 % reflectance within the two reflection bands, which has potentially led to sub-optimal colours and cell efficiencies in their case. Here, were keep reflectance at 100 % within the bands to assure minimal photocurrent losses.[34]

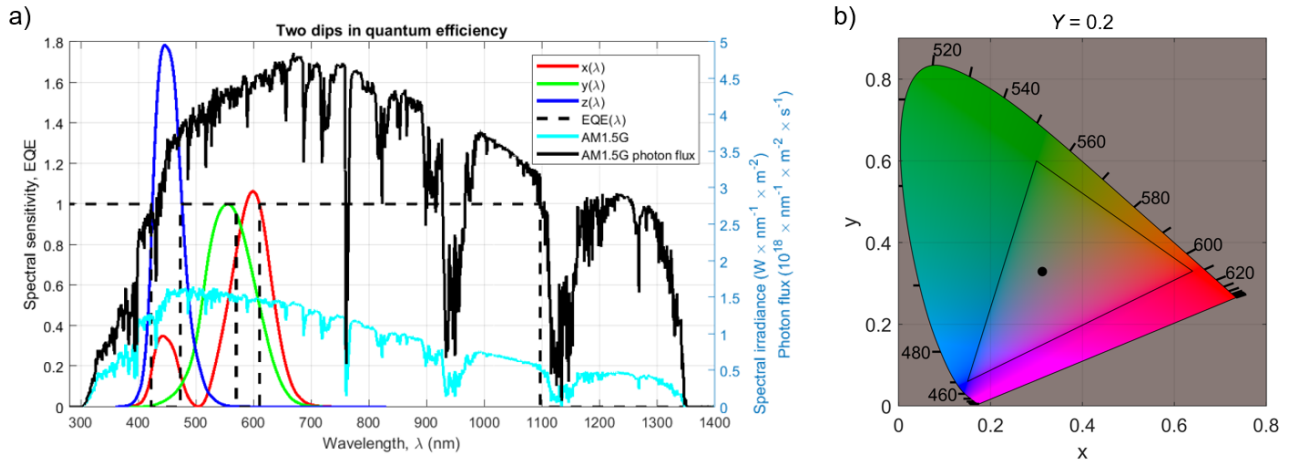


Fig. 2. a) The CIE 1931 $\bar{x}$, $\bar{y}$ and $\bar{z}$ colour matching functions, the AM1.5G spectrum both for intensity and photon flux, and an example external quantum efficiency (*EQE*) curve of a solar cell, where the colour of the cell is produced with two reflection bands within the visible wavelength region, corresponding to step-like dips in the *EQE*. The dips are defined by lower and higher cut-off limits, and zero *EQE* between them. Outside the dips, *EQE* = 1 and *R* = 0, except that *EQE* = 0 for all photon energies below the band-gap energy $E_g$ ($\lambda > \lambda_g$). b) The CIE 1931 colour space *xy* chromaticity diagram showing colours with fixed relative luminosity *Y* = 0.2. The horse-shoe-shaped edge of the diagram consists of spectral colours produced with monochromatic light, whereas the so-called 'purple line' at the bottom of the diagram corresponds to linear combinations of colours from the red and blue ends of the visible spectrum. The triangle shows the sRGB colour space and the black dot marks the coordinates of the CIE D65 standard illuminant, i.e. the white point that corresponds to achromatic grey colours.

Two reflection bands were sufficient to produce all the colours attainable with the AM1.5G spectrum. This is consistent with the similar observation made by Peharz and Ulm regarding the reproduction of RAL colours.[34] The result may seem surprising at first, considering the fact that the human colour perception is based on three different types of colour receptors (cone cells), which are represented in the CIE 1931 model by the $\bar{x}$, $\bar{y}$ and $\bar{z}$ colour-matching functions.[45] However, it is a known from colorimetry that any colour can be presented as a linear combination of two monochromatic colours.[47] The two reflection bands represent monochromatic colours, with the correspondence being closer the narrower the bands are, i.e. the darker the colour is. In fact, colours formed otherwise in the same way as here, but with only one reflectance peak or valley in the visible region, called MacAdam limits, have maximum colour purity (saturation) for a given relative luminosity, and define a 3D colour solid that includes all colours that are physically attainable under a given illumination spectrum.[45,50–52] With the two reflection bands used here, it is possible to produce not only these MacAdam limits, but also all the colours enclosed by them, and hence, all colours physically attainable under the AM1.5G spectrum.

The abovementioned insight guided an iterative optimization routine for the colour formation: First, one narrow band was placed at the peak of the $\bar{z}/\lambda$ function, as this is the most efficient way to produce the *Z* coordinate.[47] The other band was placed near the overlapping $\bar{x}$ and $\bar{y}$ functions, in a position that produced the *X* and *Y* coordinates at the correct proportions. Both bands were thereafter widened until all the coordinates *X*, *Y* and *Z* were close to their pre-determined values. The relative error between the target colour and the colour produced by the optimization procedure, $C_{error}$, was determined as

$$C_{error} = \frac{|\Delta X|+|\Delta Y|+|\Delta Z|}{X+Y+Z} \quad (15)$$

where $\Delta X$, $\Delta Y$ and $\Delta Z$ are the differences between the produced and the target $XYZ$-coordinates. The colour optimization process is described in more detail in the Electronic Supplementary Information.

Finally, the theoretical efficiency limit corresponding to each colour was obtained by finding the band-gap energy $E_g$ (used in equations 2 and 7) and the operating voltage $V$ that maximized the cell efficiency (equation 8). Optimizing the band-gap separately after forming the colour was possible, because the optimal band-gap was always outside the visible region (Fig. 2a).

# Results and discussion

## Theoretical efficiency limits

Fig. 3a-c show the theoretical efficiency limits of different solar cell colours for three different levels of relative luminosity: $Y$ = 0.25, 0.50 and 0.75. Fig. 3a shows that almost the entire sRGB colour space can be covered with a theoretical efficiency limit of over 29% when $Y$ = 0.25 (Fig. 3a). At a constant relative luminosity, yellow-green colours give the highest efficiencies. Efficiency decreases towards the blue and red corners of the CIE colour space and the purple line that represents their linear combinations (so-called non-spectral colours). For $Y$ = 0.25, the efficiencies range overall from 28 % to more than 32 %, being above 30 % for all green and yellow hues, but fall rapidly from 30 % to less than 28 % when moving toward the red and blue ends of the colour spectrum (Fig. 3a). The efficiencies are high overall mainly due to a large contribution from the near-infrared photons, augmented by a significant colour-dependent contribution from the visible region (Fig. 3a).

The superiority of the yellow-green colour is a consequence of the wavelength sensitivity of human visual perception, which is characterized by the CIE photopic luminosity function $\bar{y}$ shown in Fig. 2a. The yellow-green colour gives the highest efficiency because the human eye is most sensitive to the wavelengths that produce green and yellow colour sensations. When the colour is formed by light at around this peak sensitivity, more precisely at 550 nm, where $\bar{y}/\lambda$ has its maximum, a minimal amount of the incident photon flux is used for colour formation, leaving a maximal amount to be converted into photocurrent in the solar cell. Indeed, the calculated theoretical efficiency limit reaches its maximum when the colour approaches the 550 nm point at the monochromatic edge of the CIE chromaticity diagram (Fig. 3a-c). This is obtained by merging the two reflection bands into a single band centred at 550 nm while keeping the combined band as narrow as possible.

Note how the gamut of possible colours decreases gradually as relative luminosity increases (Fig. 3a-c). As mentioned in the previous section, the border of the gamut consists of points called MacAdam limits, and encloses all colours that are physically attainable under a given illumination spectrum.[45,50–52] Similarly, the contours of the constant-efficiency and short-circuit current density correspond roughly to the contours of constant maximum attainable luminous efficiency.[45,47] The gamut of possible colours decreases because the fixed relative luminosity sets a limit to how narrow the reflection bands can be while producing the required, fixed $Y$ value under the finite spectral irradiance of the AM1.5G illumination. When relative luminosity is increased from 0.25 to 0.50 and then 0.75 (Fig. 3a-c), the reds and blues become gradually impossible to attain, leaving mainly greens and yellows, and the colours near the white point, possible. This occurs because high relative luminosity requires wide band reflection around the human eye's peak sensitivity, which leads to bright green, yellow or grey colours.

Because brighter colours correspond to greater light reflectance, their efficiency limits are lower, ranging from ca 27 % to 30 % for $Y$ = 0.50 (Fig. 3b) and from 25 % to 28 % for $Y$ = 0.75 (Fig. 3c). To investigate the relation between colour brightness and efficiency in more detail, the theoretical efficiency limits of selected example colours are shown as a function of relative luminosity in Fig. 4. For the examples, we chose the

colour coordinates of the colour patches in the Macbeth ColorChecker chart (Fig. 5) that is a widely used as a reference target in professional colour photography and reproduction.[53] Fig. 4b shows that the efficiency of all the colours decreases with increasing relative luminosity, starting with a common value at $Y = 0$ that corresponds to an ideal black solar cell. The theoretical efficiency limit for the black cell is 33.77 %, which is equal to the value calculated by Rühle with same assumption and conditions as those used here (AM1.5G 1000 W/m$^2$, 25 °C, ideal back-reflector).[37] Note that this value is higher than the 33.1 % limit for semi-transparent cells at the black limit, because semi-transparent cells assume no back-reflector.[35,37]

The efficiency limits first decrease roughly linearly with *Y*, then drop non-linearly at higher *Y* values (Fig. 4b). This non-linearity comes from the shape of the colour-matching functions: At the lowest relative luminosity limit, the two reflectance bands are narrow and located at wavelengths where the colour matching functions take their highest values at the correct ratio. When *Y* is increased, the bands widen, which decreases the average value of the colour-matching functions within them, leading to more photons being consumed to generate the same colour chromaticity.

The efficiency limits of the original colours of the Macbeth ColorChecker chart are shown in Fig. 5. The coloured patches have efficiency limits of between 28.9 % and 32.9 %, whereas the neutral colours (grey) range between 24.1 % ($Y = 0.909$) and 33.4 % ($Y = 0.032$). The fact that the purple patch ($Y = 0.064$) has the highest and the yellow patch ($Y = 0.607$) has the lowest efficiency among all the coloured patches, although the opposite would be expected based on their chromaticity, is explained by their different *Y* values, demonstrating that, for photovoltaic efficiency, colour brightness is generally more important than chromaticity.

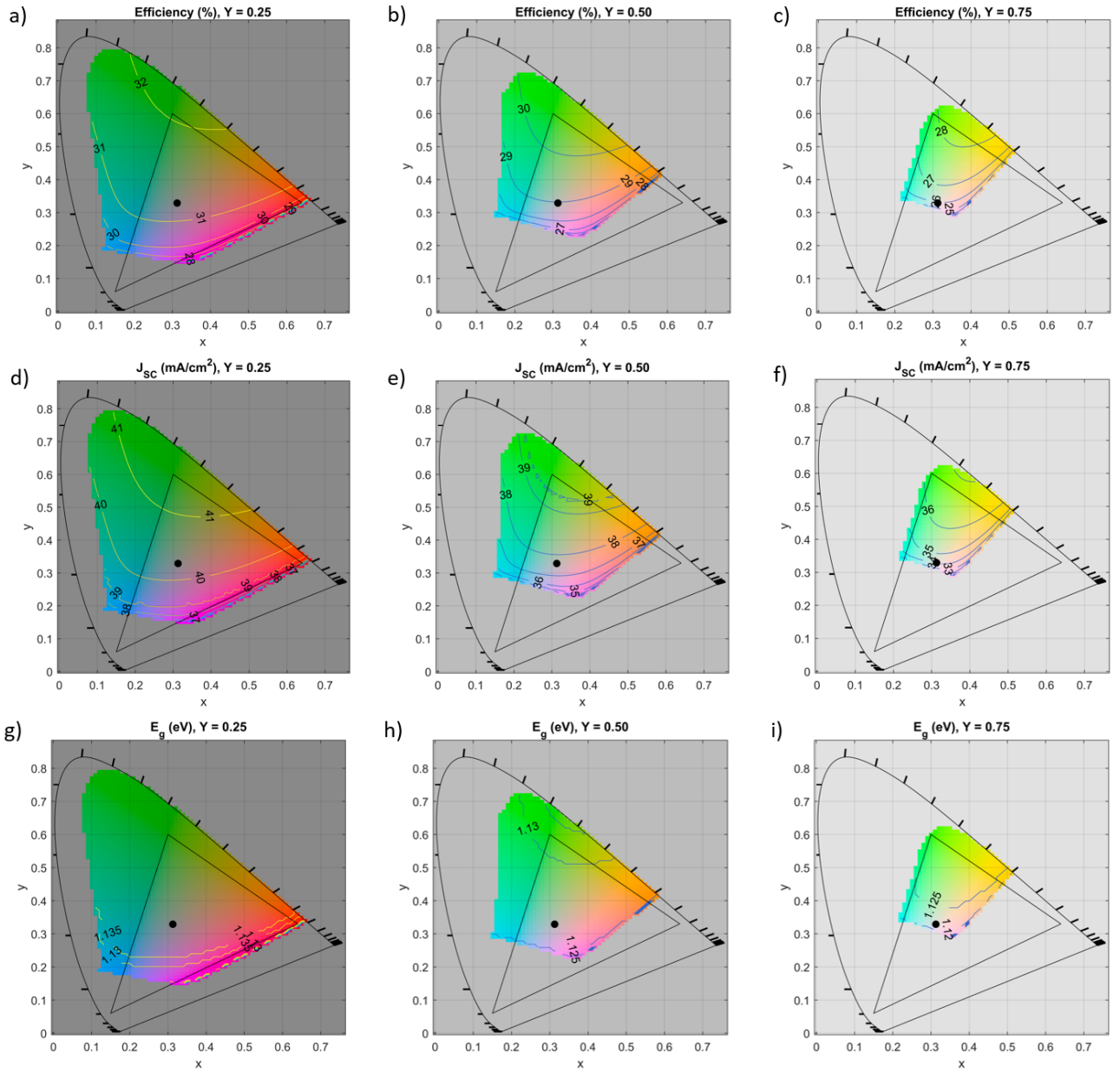


Fig. 3. Theoretical efficiency limits $\eta$ (a-c), and the corresponding short-circuit current densities $J_{SC}$ (d-f) and optimal band-gap energy $E_g$ (g-i) calculated for coloured opaque single-band-gap solar cells under standard test conditions (AM1.5G spectrum, 1000 W/m$^2$, 25 °C). The values are shown as contours over the corresponding colours in the CIE 1931 colour space chromaticity diagram. Figures are shown for three different values of relative luminosity: $Y$ = 0.25, 0.50 and 0.75. The grey background colour in each figure is that of the CIE D65 standard illuminant of the corresponding $Y$ value, marked with a black dot in the diagram. The sRGB colour space is marked with a triangle. Only colours that have a relative error less than 0.5 % are shown.

Comparing the different colours with the achromatic grey, it is observed that the greens and yellows have a generally higher efficiency, and the blues, reds and purples have a lower efficiency, than grey (Fig. 4b). This is because producing a grey colour requires some reflectance in the red and blue wavelength region, where photopic sensitivity is lower than in the yellow-green region. In this sense, highly saturated purple colours are the most inefficient colours as they combine the least efficient ends of the visible spectrum. On the other hand, bright saturated blues are the most difficult colours to produce by sunlight reflection. For example, at $Y = 0.25$, all the other colours in the sRGB colour space can be produced, except those in the blue corner (Fig. 3a). This is because the blue colour matching function $\bar{z}$ overlaps much less with the luminosity function $\bar{y}$ than the red colour matching function $\bar{x}$ does (Fig. 2a). From this perspective, it is an interesting coincidence that commercial multi-crystalline silicon solar cells are often blue-tinted by the design of their anti-reflection coating.[13] Striking the best compromise between colour and efficiency has clearly not been the primary target of their performance optimization. We note that Peharz and Ulm arrived at different conclusions on the trade-off between "strong colour perception" and photovoltaic losses, because they did not compare the efficiency of different colours at equal relative luminosity.[34] Although not discussed by Peharz and Ulm, the validity of our conclusion can be qualitatively observed in their results (Fig. 4 in ref [34]): the power loss is least for yellow-green colours and increases towards the blue and red ends of the spectrum, when colours of similar brightness appearance are compared.

## Optimal band-gap energy and current – voltage characteristics

Fig. 3 and Fig. 4 illustrate how the optimal band-gap energy $E_g$ and the current – voltage characteristics $J_{SC}$, $V_{OC}$ and *FF* of an optimized solar cell depend on its colour. Corresponding figures for $J_{MPP}$ and $V_{MPP}$ are provided as Electronic Supplementary Information. As thoroughly explained above, colour affects cell efficiency mainly through its impact on photocurrent generation. This can be clearly seen in the CIE chromaticity diagrams (Fig. 3), as well as in Fig. 4, where $J_{SC}$ shows a similar colour-dependence as efficiency, whereas $E_g$, $V_{OC}$ and *FF* only vary slightly with chromaticity and relative luminosity. The small variations in $V_{OC}$ and *FF* follow the trends in $J_{SC}$ as dictated by the diode model (equations 1 and 5 – 7), whereas the weak colour-dependence of the optimal $E_g$ is a result of it always being far from the visible region (Fig. 2a). The small colour-variation in $E_g$ follows essentially from the availability of sub-$E_g$ photons: the higher is optimal $E_g$, the higher the absorbed photon flux below $E_g$, and therefore it is maximal for those yellow-green colours that require least photons to produce.

The only larger variation is a step-wise change in the optimal band-gap energy at relative luminosity values between 0.05 and 0.15 (Fig. 4d). A corresponding step is seen in $J_{SC}$, $V_{OC}$ and *FF* (Fig. 4c, e and f), however, efficiency varies smoothly (Fig. 4b), because the steps in $J_{SC}$, $V_{OC}$ and *FF* compensate each other. The abrupt change in the optimal $E_g$ is also visible in Lunt's results[35] and is caused by local maxima in the efficiency vs. $E_g$ curves[37]. The local maxima are produced by atmospheric absorption bands in the AM1.5G spectrum, starting at ca 930 and 1100 nm (Fig. 2a). Optimization between high band-gap energy (high $V_{OC}$, low $\lambda_g$) and high photocurrent density (high $J_{SC}$, high $\lambda_g$) leads to optimal $E_g$ values that correspond to placing $\lambda_g$ right at the edge of these absorption bands, depending on how high the light absorption in the visible region is. For $Y < 0.15$, high visible light absorptance favours less absorption in the NIR region allowing a higher $E_g$, which sets the optimal $E_g$ at 1.337 eV ($\lambda_g$ = 927 nm), yielding $V_{OC}$ = 1.08 V and $J_{SC} < 35$ mA cm$^{-2}$ (Fig. 4c and d). For $Y >$ 0.15, visible light absorption is weaker, favouring more NIR absorption, which causes the optimal $E_g$ values to drop between 1.115 eV and 1.135 eV ($\lambda_g$ = 1092 … 1112 nm), producing $V_{OC}$ between 0.866 V and 0.892 V, and $J_{SC}$ between 30 mA cm$^{-2}$ and 42 mA cm$^{-2}$, depending on the colour and its brightness. Note how the optimal $\lambda_g$ values coincide with the drops in the AM1.5G spectrum at ca 930 nm and 1100 nm, as already mentioned (Fig. 2a). We can thus conclude that the optimal band-gap energy for theoretically ideal coloured

solar cells is ca 1.1 eV ($\lambda_g$ = 1100 nm), whereas for black or dark cells it is 1.337 eV ($\lambda_g$ = 927 nm). These values are close to those found by Lunt for semi-transparent achromatic solar cells[35]. Note that the optimal band-gap of coloured solar cells, almost perfectly matches the 1.12 eV band-gap of crystalline silicon, suggesting that, crystalline silicon is, band-gap-wise, close to an ideal photovoltaic material for opaque coloured photovoltaics.

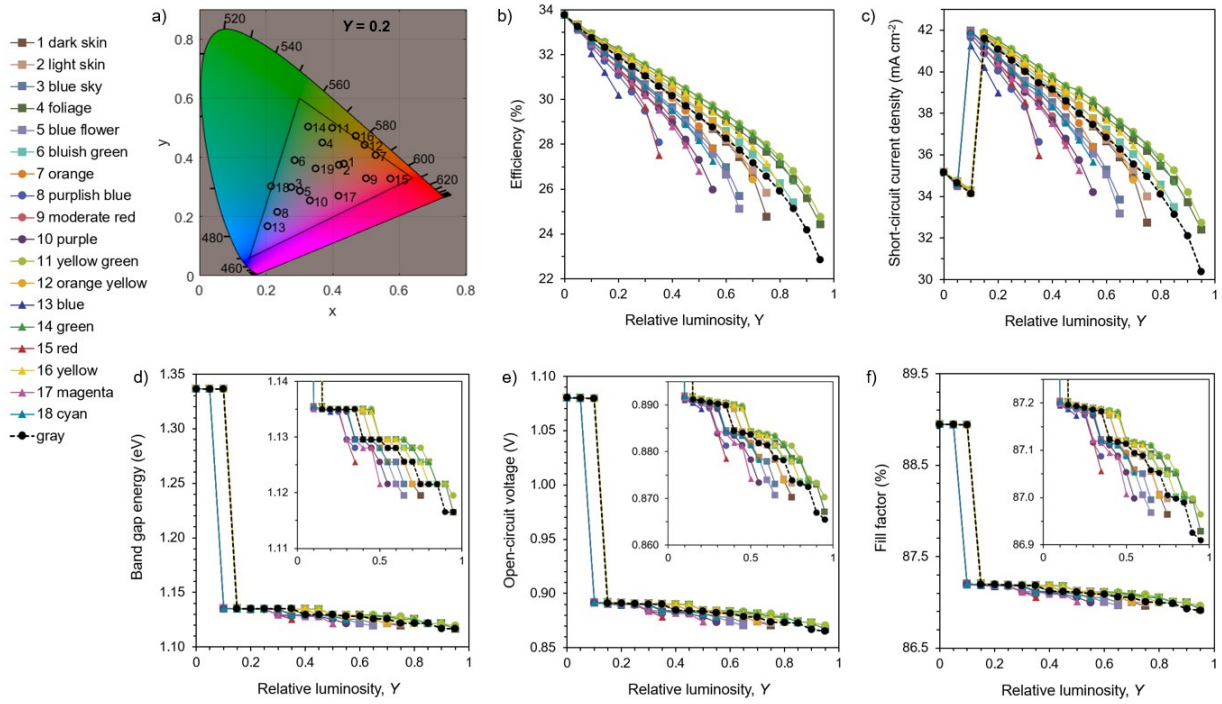


Fig. 4. The figure shows the effect of colour brightness (relative luminosity, *Y*) on the theoretical efficiency limits (b), optimal band-gap energy (d), and current-voltage characteristics (c, e, f) for 19 example colours distributed in the CIE chromaticity diagram as shown in panel (a). The example colours correspond to the colour patches of the Macbeth ColorChecker chart shown in Fig. 5. The relative luminosity *Y* was varied between 0 and 0.95 in 0.05 steps. Only colours that were produced with a relative error less than 0.5 % are shown.

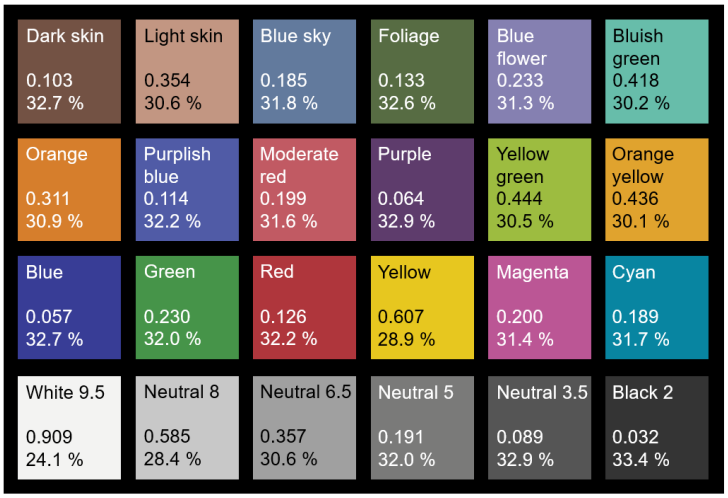


Fig. 5. Theoretical efficiency limits of colours corresponding to the colour patches of the Macbeth ColorChecker chart, calculated based on the "BabelColor Avg." xyY data obtained from Pascale.[53] The *Y* value of each colour is shown above its efficiency limit, using AM1.5G as the illuminant (1000 W/m$^2$, 25 °C). The

bottom row consists of neutral (grey) colours between 9.5 and 2 in Munsell value (lightness). For reference, the efficiency limit for the fully black colour between the patches is 33.77 %. The colours were reproduced for the figure using the original sRGB coordinates provided by GretagMacbeth for D50 standard illuminant.[53] The relative error of colour $C_{error}$ was less than 0.53 % in all cases. The complete data including optimal band-gap and current – voltage characteristics is shown in Table 1.

Table 1. Theoretical efficiency limits of colours corresponding to the colour patches of the Macbeth ColorChecker chart (Fig. 5). The xyY coordinates are the "BabelColor Avg." data obtained from Pascale (2006)[53], which were originally obtained as an average of 20 different real ColorChecker charts. The photovoltaic data corresponding to the xyY coordinates were obtained using AM1.5G as the illuminant 1000 W/m$^2$, 25 °C).

| Colour | x | y | Y | $\eta$ (%) | $J_{SC}$ (mA/cm$^2$) | $V_{OC}$ (V) | $FF$ (%) | $E_g$ (eV) | $J_{MPP}$ (mA/cm$^2$) | $V_{MPP}$ (V) | $C_{error}$ (%) |
|---|---|---|---|---|---|---|---|---|---|---|---|
| **1 dark skin** | 0.4336 | 0.3787 | 0.1029 | 32.74 | 34.12 | 1.0794 | 88.94 | 1.337 | 33.25 | 0.9851 | 0.010 |
| **2 light skin** | 0.4187 | 0.3749 | 0.3540 | 30.60 | 39.46 | 0.8899 | 87.18 | 1.135 | 38.23 | 0.8007 | 0.049 |
| **3 blue sky** | 0.2757 | 0.2996 | 0.1849 | 31.81 | 40.97 | 0.8909 | 87.19 | 1.135 | 39.70 | 0.8017 | 0.013 |
| **4 foliage** | 0.3688 | 0.4501 | 0.1329 | 32.63 | 41.96 | 0.8920 | 87.20 | 1.136 | 40.66 | 0.8027 | 0.052 |
| **5 blue flower** | 0.3016 | 0.2871 | 0.2328 | 31.28 | 40.30 | 0.8904 | 87.19 | 1.135 | 39.05 | 0.8013 | 0.038 |
| **6 bluish green** | 0.2856 | 0.3905 | 0.4175 | 30.20 | 38.98 | 0.8891 | 87.17 | 1.135 | 37.77 | 0.8000 | 0.015 |
| **7 orange** | 0.5291 | 0.4081 | 0.3106 | 30.95 | 39.89 | 0.8902 | 87.18 | 1.135 | 38.65 | 0.8010 | 0.015 |
| **8 purplish blue** | 0.2335 | 0.2157 | 0.1136 | 32.18 | 41.42 | 0.8912 | 87.20 | 1.135 | 40.14 | 0.8019 | 0.062 |
| **9 moderate red** | 0.5002 | 0.3295 | 0.1989 | 31.60 | 40.71 | 0.8907 | 87.19 | 1.135 | 39.44 | 0.8015 | 0.028 |
| **10 purple** | 0.3316 | 0.2544 | 0.0639 | 32.92 | 34.30 | 1.0796 | 88.94 | 1.337 | 33.43 | 0.9852 | 0.149 |
| **11 yellow green** | 0.3986 | 0.5002 | 0.4440 | 30.54 | 39.38 | 0.8899 | 87.18 | 1.135 | 38.15 | 0.8007 | 0.035 |
| **12 orange yellow** | 0.4960 | 0.4426 | 0.4360 | 30.15 | 39.14 | 0.8844 | 87.12 | 1.130 | 37.92 | 0.7954 | 0.011 |
| **13 blue** | 0.2042 | 0.1676 | 0.0570 | 32.71 | 34.08 | 1.0794 | 88.94 | 1.337 | 33.22 | 0.9851 | 0.530 |
| **14 green** | 0.3262 | 0.5040 | 0.2297 | 32.03 | 41.25 | 0.8910 | 87.19 | 1.135 | 39.97 | 0.8018 | 0.026 |
| **15 red** | 0.5734 | 0.3284 | 0.1262 | 32.20 | 41.45 | 0.8912 | 87.20 | 1.135 | 40.16 | 0.8020 | 0.070 |
| **16 yellow** | 0.4693 | 0.4730 | 0.6072 | 28.91 | 37.58 | 0.8834 | 87.11 | 1.130 | 36.40 | 0.7944 | 0.017 |
| **17 magenta** | 0.4175 | 0.2702 | 0.1998 | 31.36 | 40.41 | 0.8905 | 87.19 | 1.135 | 39.15 | 0.8013 | 0.019 |
| **18 cyan** | 0.2146 | 0.3028 | 0.1889 | 31.73 | 40.87 | 0.8908 | 87.19 | 1.135 | 39.60 | 0.8016 | 0.038 |
| **19 white 9.5** | 0.3486 | 0.3625 | 0.9094 | 24.09 | 31.98 | 0.8668 | 86.92 | 1.117 | 30.96 | 0.7784 | 0.007 |
| **20 neutral 8** | 0.3451 | 0.3593 | 0.5850 | 28.44 | 37.06 | 0.8816 | 87.09 | 1.128 | 35.89 | 0.7927 | 0.015 |
| **21 neutral 6.5** | 0.3447 | 0.3588 | 0.3571 | 30.55 | 39.40 | 0.8899 | 87.18 | 1.135 | 38.17 | 0.8007 | 0.014 |
| **22 neutral 5** | 0.3433 | 0.3586 | 0.1912 | 31.98 | 41.18 | 0.8910 | 87.19 | 1.135 | 39.90 | 0.8018 | 0.043 |
| **23 neutral 3.5** | 0.3425 | 0.3577 | 0.0887 | 32.87 | 34.24 | 1.0795 | 88.94 | 1.337 | 33.37 | 0.9852 | 0.133 |
| **24 black 2** | 0.3436 | 0.3562 | 0.0317 | 33.45 | 34.83 | 1.0800 | 88.94 | 1.337 | 33.95 | 0.9856 | 0.364 |

## Interpretation, validity and practical relevance of the results

**Interpretation of the colours reproduced in this paper**

It is important to note that the visual perception of the colours shown in all the figures of this paper depends on the device, format (digital, print or other), and the illumination spectrum used for their reproduction or viewing. Most importantly, none of the colours outside the sRGB color space, marked with a triangle in the figures, appear correctly because they have been mapped into the sRGB space. The result of mapping the CIE XYZ-coordinates into the sRGB space also depends on the chosen standard white, which in this work was the D65 spectrum.

Note also that the grey colour is produced here with two reflection bands that may have a gap between them in the visible region, especially at low *Y* values when the bands are narrow. The grey colours reported here do not therefore represent spectrally flat reflective surfaces – white light reflected from them could have a low colour rendering index (CRI). Grey colours with higher CRI could be obtained by using one instead of two reflection bands, however, their efficiency limits are equal or lower than those obtained with two bands and are therefore omitted in the present discussion.

**Validity of the results for different illumination conditions**

The absolute theoretical efficiencies calculated here are valid only for solar cells that are operated and viewed under the standard test conditions (AM1.5G spectrum, 1000 W/m$^2$, 25 °C). Small natural variations in the sunlight spectrum, due for example to cloud cover, humidity, diffuse and ground-reflected radiation and time of day that are omitted here, are not expected to change the relative efficiency of different colours much. However, artificial “white light” sources that have a spectral irradiance markedly different from the sunlight spectrum, for example white LED and fluorescent light, would favour colours produced with reflection bands near the spectral peaks of the source spectrum over colours produced with wavelengths located in the spectral valleys. When it comes to temperature-dependence, it can be seen from the physical model that the cell temperature should not change the relative efficiency of different colours, because it affects only the recombination current (eqs. 5 – 7) and not at all the photocurrent (eqs. 2 and 4) that almost exclusively determines the colour dependence of the results. The model calculations confirm this expectation (Figure S4 in Supplementary Information).

**Validity of the results for different angular reflectance distributions**

The comparison of the efficiencies of different solar cell colours assumes that all the colours have been produced with an equal angular reflectance distribution function. The reflectance distribution does not have to be angle-independent (Lambertian), but must be same for all compared coloured surfaces, including the white surface that is used as a reference for the relative luminosity (*Y* = 1). This requirement is essential, because the reflectance used in the efficiency calculations refers to the total hemispherical reflectance. For example, if two diffusively reflective coloured surfaces had different angular reflectance distributions, their relative brightness would depend on the viewing angle, making their quantitative colour-efficiency comparison ambiguous from the observer’s point-of-view. For the same reason, the results do not apply for solar cells with iridescent colours, because iridescent surfaces do not have an unambiguous colour that the efficiency limit could be ascribed to.

**Relevance of the results to practical coloured surfaces**

Reflecting two sharp and narrow wavelength bands is an extreme ideal scenario that practical coloured surfaces, characterized by broadband reflectance, can approach, but never reach exactly. For example, if the measured reflectance spectra of the physical Macbeth ColorChecker targets had been used in the calculations, the efficiency limits would have been lower than the values shown in Fig. 5, like observed by

Peharz and Ulm in the case of RAL colours.[34] Furthermore, the practical efficiencies of coloured solar cells are expected to be much lower than these theoretical limits, because even the record efficiencies of black solar cells are below them, and any parasitic light absorption further decreases the cell efficiencies. How closely real coloured surfaces can approach the performance provided by the theoretically optimal two reflection bands will depend on their materials and structure. This offers an interesting topic for further research. Non-iridescent structural colours that can be realized by combining the effects of light interference and diffuse light scattering[21,22,26,27] are particularly promising, because they offer a way to minimize parasitic light absorption while producing diffuse, matt colours important in design and architecture. For example, Escarré et al. reported white solar modules with 11.4 % efficiency based on silicon heterojunction solar cells, representing 40 % power loss compared to the standard black solar modules of the same type.[27] Jolissaint et al. reported blue and orange Kromatix solar modules with matt appearance and more than 17 % efficiency, showing less than 7 % power loss due to coloration.[26] Also, Neder et al. reached relatively low, less than 14 %, power loss in green silicon solar modules with resonant dielectric nanoscatterers fabricated on the module cover slides.[22]

Overall, the relative power loss due to coloration of solar cells has been less than 15 % in the best reported cases.[12–15,22,23,25–27,29,31] However, comparison of the results between different studies is difficult because the studied colours have differed both in chromaticity and brightness, which both have significant, fundamental influence on the solar cell efficiency, as Fig. 4 shows. We suggest that the colours of the Macbeth ColorChecker chart, with their efficiency limits (Fig. 5) and current-voltage characteristics (Table 1), could be used as a common point of reference for quantitative comparison of different experimental strategies for solar cell colour production and optimization.

**The most efficient colour for solar cells is the colour of green leaves**

The results of this paper show that the most efficient colours for a solar cell are spectral yellow-green colours near 550 nm, which is close to the colour of green leaves. We arrive at this conclusion by acknowledging that all colours become equally efficient, and black, when their luminosity is zero (Fig. 4b). It is hard to ignore the poetical aspects of this result, bearing in mind that photovoltaics is portrayed as “green” technology and solar cells used in photoelectrochemical energy conversion are known as “artificial leaves”. The connection comes from the complementary spectral sensitivity of photosynthesis and human visual perception. Whilst perhaps coincidental, it appears that human visual aesthetics are in spectral harmony both with photosynthetic plants and photovoltaic technology.[54]

## Conclusions

We calculated the theoretical efficiency limits of coloured opaque single-band-gap solar cells and studied the interplay between colour and photovoltaic performance. A broad range of colours with high photovoltaic efficiency is possible, because an optimally-coloured solar cell utilizes the near-infrared light between 700 nm and 1100 nm wavelengths efficiently, and only a small fraction of the visible light between 400 nm and 700 nm is required to produce typical colours. Almost all sRGB colours can be formed with more than 29 % theoretical efficiency when their relative luminosity is less than 0.25, which corresponds to less than a 14 % relative performance loss compared to an ideal black solar cell. This optical loss depends more on the relative luminosity (brightness) of the colour, than its chromaticity (hue and colourfulness). Nevertheless, yellow-green is the most efficient photovoltaic colour, because human eye is most sensitive to the yellow-green wavelengths near 550 nm. We hope that these results inspire and encourage the development of the next generation of performance-optimized, aesthetic building- and product-integrated photovoltaics. The efficiency limits of the colours in the MacBeth ColorChecker chart may be used as a common point of reference for this purpose.

**Conflicts of interest**

There are no conflicts of interest to declare

**References**


1. Ballif C, Perret-Aebi L-E, Lufkin S, Rey E. Integrated thinking for photovoltaics in buildings. *Nat Energy*. 2018;3(6):438-442. doi:10.1038/s41560-018-0176-2

2. Heinstein P, Ballif C, Perret-Aebi L-E. Building integrated photovoltaics (BIPV): review, potentials, barriers and myths. *Green*. 2013;3(2):125–156.

3. Hille SL, Curtius HC, Wüstenhagen R. Red is the new blue – The role of color, building integration and country-of-origin in homeowners' preferences for residential photovoltaics. *Energy Build*. 2018;162:21-31. doi:10.1016/j.enbuild.2017.11.070

4. Reich NH, Veefkind M, Sark WGJHM van, Alsema EA, Turkenburg WC, Silvester S. A solar powered wireless computer mouse: Industrial design concepts. *Sol Energy*. 2009;83(2):202-210. doi:10.1016/j.solener.2008.07.022

5. Apostolou G, Reinders AHME. Overview of Design Issues in Product-Integrated Photovoltaics. *Energy Technol*. 2014;2(3):229-242. doi:10.1002/ente.201300158

6. Ameri T, Dennler G, Waldauf C, et al. Fabrication, Optical Modeling, and Color Characterization of Semitransparent Bulk-Heterojunction Organic Solar Cells in an Inverted Structure. *Adv Funct Mater*. 2010;20(10):1592-1598. doi:10.1002/adfm.201000176

7. Fakharuddin A, Jose R, Brown TM, Fabregat-Santiago F, Bisquert J. A perspective on the production of dye-sensitized solar modules. *Energy Environ Sci*. 2014;7(12):3952-3981. doi:10.1039/C4EE01724B

8. Ren Y, Sun D, Cao Y, et al. A Stable Blue Photosensitizer for Color Palette of Dye-Sensitized Solar Cells Reaching 12.6% Efficiency. *J Am Chem Soc*. 2018;140(7):2405-2408. doi:10.1021/jacs.7b12348

9. Ghufran Hashmi S, Özkan M, Halme J, et al. Dye-sensitized solar cells with inkjet-printed dyes. *Energy Environ Sci*. 2016;9(7):2453-2462. doi:10.1039/C6EE00826G

10. E. Calvo M. Materials chemistry approaches to the control of the optical features of perovskite solar cells. *J Mater Chem A*. 2017;5(39):20561-20578. doi:10.1039/C7TA05666D

11. Noh JH, Im SH, Heo JH, Mandal TN, Seok SI. Chemical Management for Colorful, Efficient, and Stable Inorganic–Organic Hybrid Nanostructured Solar Cells. *Nano Lett*. 2013;13(4):1764-1769. doi:10.1021/nl400349b

12. Selj JH, Mongstad TT, Søndenå R, Marstein ES. Reduction of optical losses in colored solar cells with multilayer antireflection coatings. *Sol Energy Mater Sol Cells*. 2011;95(9):2576-2582. doi:10.1016/j.solmat.2011.03.005

13. Li M, Zeng L, Chen Y, Zhuang L, Wang X, Shen H. Realization of Colored Multicrystalline Silicon Solar Cells with SiO2/SiNx:H Double Layer Antireflection Coatings. *Int J Photoenergy*. 2013;2013. doi:10.1155/2013/352473

14. Tobias I, Moussaoni AE, Luque A. Colored solar cells with minimal current mismatch. *IEEE Trans Electron Devices*. 1999;46(9):1858-1865. doi:10.1109/16.784185

15. Yoo GY, Jeong J, Lee S, et al. Multiple-Color-Generating Cu(In,Ga)(S,Se)2 Thin-Film Solar Cells via Dichroic Film Incorporation for Power-Generating Window Applications. *ACS Appl Mater Interfaces*. 2017;9(17):14817-14826. doi:10.1021/acsami.7b01416

16. Klampaftis E, Ross D, Richards BS. Color, graphic design and high efficiency for photovoltaic modules. In: *2014 IEEE 40th Photovoltaic Specialist Conference (PVSC)*. ; 2014:0025-0029. doi:10.1109/PVSC.2014.6925025

17. Tai Q, Yan F. Emerging Semitransparent Solar Cells: Materials and Device Design. *Adv Mater*. 29(34):1700192. doi:10.1002/adma.201700192

18. Sun J, Jasieniak JJ. Semi-transparent solar cells. *J Phys Appl Phys*. 2017;50(9):093001. doi:10.1088/1361-6463/aa53d7

19. Traverse CJ, Pandey R, Barr MC, Lunt RR. Emergence of highly transparent photovoltaics for distributed applications. *Nat Energy*. 2017;2(11):849-860. doi:10.1038/s41560-017-0016-9

20. Lynn N, Mohanty L, Wittkopf S. Color rendering properties of semi-transparent thin-film PV modules. *Build Environ*. 2012;54:148-158. doi:10.1016/j.buildenv.2012.02.010

21. Bläsi B, Kroyer T, Höhn O, et al. Morpho Butterfly Inspired Coloured BIPV Modules. In: *33rd European PV Solar Energy Conference and Exhibition*. ; 2017.

22. Neder V, Luxembourg SL, Polman A. Efficient colored silicon solar modules using integrated resonant dielectric nanoscatterers. *Appl Phys Lett*. 2017;111(7):073902. doi:10.1063/1.4986796

23. Peharz G, Berger K, Kubicek B, et al. Application of plasmonic coloring for making building integrated PV modules comprising of green solar cells. *Renew Energy*. 2017;109:542-550. doi:10.1016/j.renene.2017.03.068

24. Lee K-T, Lee JY, Xu T, Park HJ, Guo LJ. Colored dual-functional photovoltaic cells. *J Opt*. 2016;18(6):064003. doi:10.1088/2040-8978/18/6/064003

25. Pélisset S, Joly M, Chapuis V, et al. Efficiency of silicon thin-film photovoltaic modules with a front coloured glass. *Proceeding CISBAT Int Conf 2011*. 2011:37-42. https://infoscience.epfl.ch/record/170333. Accessed June 22, 2017.

26. Jolissaint N, Hanbali R, Hadorn J-C, Schüler A. Colored solar façades for buildings. *Energy Procedia*. 2017;122:175-180. doi:10.1016/j.egypro.2017.07.340

27. Escarré J, Li HY, Sansonnens L, et al. When PV modules are becoming real building elements: White solar module, a revolution for BIPV. In: *2015 IEEE 42nd Photovoltaic Specialist Conference (PVSC)*. ; 2015:1-2. doi:10.1109/PVSC.2015.7355630

28. Schregle R, Krehel M, Wittkopf S. Computational Colour Matching of Laminated Photovoltaic Modules for Building Envelopes. *Buildings*. 2017;7(3):72.

29. Slooff LH, Roosmalen J van, Okel LAG, et al. An architectural approach for improving aesthetics of PV. *Present EUPVSEC*. 2017;25:29.

30. Schregle R, Wittkopf S. An Image-Based Gamut Analysis of Translucent Digital Ceramic Prints for Coloured Photovoltaic Modules. *Buildings*. 2018;8(2):30.

31. Lien S-Y. Artist Photovoltaic Modules. *Energies*. 2016;9(7):551. doi:10.3390/en9070551

32. Moor T, Egloff B, Tomovic T, Wittkopf S. REPEAT – Textile Design for PV Modules! Design-driven Strategies for Photovoltaic Modules. *Des J*. 2017;20(sup1):S1879-S1893. doi:10.1080/14606925.2017.1352706

33. Forberich K, Guo F, Bronnbauer C, Brabec CJ. Efficiency Limits and Color of Semitransparent Organic Solar Cells for Application in Building-Integrated Photovoltaics. *Energy Technol*. 2015;3(10):1051-1058. doi:10.1002/ente.201500131

34. Peharz G, Ulm A. Quantifying the influence of colors on the performance of c-Si photovoltaic devices. *Renew Energy*. 2018;129:299-308. doi:10.1016/j.renene.2018.05.068

35. Lunt RR. Theoretical limits for visibly transparent photovoltaics. *Appl Phys Lett*. July 2012. doi:10.1063/1.4738896

36. Shockley W, Queisser HJ. Detailed Balance Limit of Efficiency of p-n Junction Solar Cells. *J Appl Phys*. 1961;32(3):510-519. doi:10.1063/1.1736034

37. Rühle S. Tabulated values of the Shockley–Queisser limit for single junction solar cells. *Sol Energy*. 2016;130(Supplement C):139-147. doi:10.1016/j.solener.2016.02.015

38. Goodwin H, Jellicoe TC, Davis NJLK, Böhm ML. Multiple exciton generation in quantum dot-based solar cells. *Nanophotonics*. 2018;7(1):111–126. doi:10.1515/nanoph-2017-0034

39. Trupke T, Green MA, Würfel P. Improving solar cell efficiencies by up-conversion of sub-band-gap light. *J Appl Phys*. 2002;92(7):4117-4122. doi:10.1063/1.1505677

40. Trupke T, Green MA, Würfel P. Improving solar cell efficiencies by down-conversion of high-energy photons. *J Appl Phys*. 2002;92(3):1668-1674. doi:10.1063/1.1492021

41. Luque A, Martí A. The Intermediate Band Solar Cell: Progress Toward the Realization of an Attractive Concept. *Adv Mater*. 22(2):160-174. doi:10.1002/adma.200902388

42. Kirchartz T, Rau U. Detailed balance and reciprocity in solar cells. *Phys Status Solidi A*. 205(12):2737-2751. doi:10.1002/pssa.200880458

43. Lunt RR, Osedach TP, Brown PR, Rowehl JA, Bulović V. Practical Roadmap and Limits to Nanostructured Photovoltaics. *Adv Mater*. 23(48):5712-5727. doi:10.1002/adma.201103404

44. Smith T, Guild J. The C.I.E. colorimetric standards and their use. *Trans Opt Soc*. 1931;33(3):73. doi:10.1088/1475-4878/33/3/301

45. Malacara D. *Color Vision and Colorimetry: Theory and Applications, Second Edition*. 1000 20th Street, Bellingham, WA 98227-0010 USA: SPIE; 2011. doi:10.1117/3.881172

46. Colour Matching Functions. http://cvrl.ioo.ucl.ac.uk/cmfs.htm.

47. MacAdam DL. Maximum attainable luminous efficiency of various chromaticities. *JOSA*. 1950;40(2):120–120.

48. Schrödinger E. Theorie der Pigmente von größter Leuchtkraft. *Ann Phys*. 1920;367(15):603-622. doi:10.1002/andp.19203671504

49. MacAdam DL. The Theory of the Maximum Visual Efficiency of Colored Materials. *JOSA*. 1935;25(8):249-252. doi:10.1364/JOSA.25.000249

50. Perales E, Mora Estevan T, Viqueira Pérez V, et al. *A New Algorithm for Calculating the MacAdam Limits for Any Luminance Factor, Hue Angle and Illuminant*. International Colour Association; 2005. http://rua.ua.es/dspace/handle/10045/955. Accessed May 13, 2018.

51. MacAdam DL. Maximum Visual Efficiency of Colored Materials. *JOSA*. 1935;25(11):361-367. doi:10.1364/JOSA.25.000361

52. Martínez-Verdú F, Perales E, Chorro E, Fez D de, Viqueira V, Gilabert E. Computation and visualization of the MacAdam limits for any lightness, hue angle, and light source. *JOSA A*. 2007;24(6):1501-1515. doi:10.1364/JOSAA.24.001501

53. Pascale D. RGB coordinates of the Macbeth ColorChecker. *BabelColor Co*. 2006:1–16.

54. Gençer E, Miskin C, Sun X, et al. Directing solar photons to sustainably meet food, energy, and water needs. *Sci Rep*. 2017;7. doi:10.1038/s41598-017-03437-x